THE STUDY OF TEMPERATURE RISE IN A 90-DEGREE SHARP BEND MICROCHANNEL FLOW UNDER CONSTANT WALL TEMPERATURE CONDITION

C.-Y. Huang * **C.-A. Li** **B.-H. Huang** **T.-M. Liou**

Department of Power Mechanical Engineering
National Tsing Hua University
Hsinchu, Taiwan

ABSTRACT

This study presents the fluid temperature measurement at a 90-degree sharp bend inside a microchannel using molecule-based temperature sensor technique. This technique provides both detailed and global information for temperature investigation in microfluidic research. Rhodamine B was selected as the molecule-based temperature probe in the experiment to provide non-invasive and straightforward measurements. To resolve the luminescence deviation in the microscale temperature measurements introduced by the corner structure, in-situ calibration method and pixel-by-pixel correction were applied during the data reduction. The temperature measurement was performed in a 200μm wide, 67μm deep and 2cm long PDMS microchannel with a 90-degree sharp bend at the center. The temperature profile was measured at a Reynolds number of 27.66 using Rhodamine B in DI water while the bottom of channel was heated at 50°C. As revealed by the molecule-based temperature sensor, the temperature variation along the central line increased 2°C while passing the corner. Additionally, the lateral temperature distributions upstream of the corner show the temperature increase near the outer side of microchannel and decreased near the inner side. The velocity profiles around the 90-degree sharp bend were acquired to analyze the flow after corner. Secondary flow structure after the corner was observed in the velocity profiles along the depth of the microchannel. This study analyzes the thermal flow fields in the microchannel with a 90-degree sharp bend and reveals that regardless of the low Reynolds number, the flow mixing after the corner resulted in the increase of temperature downstream of the bend.

Keywords: Temperature measurements, 90-degree sharp bend, Flow visualization, Molecule-based temperature sensor.

1. INTRODUCTION

Heat transfer enhancement in micro heat exchangers, which provides the solution of heat dissipation for high power microelectromechanical (MEMS) devices, has become an important issue to improve the performance of MEMS devices in various applications. Different designs of microchannels such as straight, 90 degree bend, and serpentine have been constructed and integrated as the components for fluid delivery as well as heat dissipation in the micro heat exchangers. The temperature variations in such microchannel designs are critical in characterizing the heat transfer in microchannel flow and evaluating further applications to the micro heat exchangers. The excessive heat generated by a MEMS device is removed by the fluid flowing in the microchannels inside a given micro heat exchanger which is attached to the back of the MEMS device. To study the temperature variation of fluid inside a microchannel, the heat removal process can be simulated as single phase heat convection with the bottom side heated thermal boundary condition, which is either constant wall heat flux or constant wall temperature. Several research groups have studied temperature variations and heat transfer inside straight or serpentine microchannels under constant wall heat flux or constant wall temperature thermal boundary conditions [1-4].

Conventional experimental approaches study the temperature distribution inside microchannels using thermocouples installed at channel inlet and exit to acquire the temperature data, and further elaborate the temperature profile inside the channel by extrapolation or through simulation [5]. In the past decade, with the advance of MEMS technology, micro-sized thermocouples have been developed and applied inside microchannels to obtain temperature data in the flow field [6]. However, the temperature measurements using micro thermocouples can only obtain limited and discrete data due to comparable sizes of micro-thermocouple and microchannel. The detailed temperature information inside the microchannel is important when investigating the temperature evolution due to different thermal

* Corresponding author (cyhuang@pme.nthu.edu.tw)

DOI : 10.1017/jmech.2014.60
Copyright © 2014 The Society of Theoretical and Applied Mechanics, R.O.C.
https://doi.org/10.1017/jmech.2014.60 Published online by Cambridge University Press

boundary conditions and different microchannel designs. Molecule-based temperature sensor technique has been applied to micro devices for acquiring detailed temperature information from microscale and unsteady flow fields in a micro turbine device [7]. This method uses luminescent molecules like Rhodamine B that changes emitted fluorescence intensity corresponded to the temperature in the environment. It is adapted from the conventional macroscale experimental technique known as Temperature-Sensitive Paint (TSP). Similar techniques like Laser-Induced Fluorescence (LIF) technique have been applied in the microfluidic research for temperature measurements and heat transfer analysis in various microchannel devices [8-11]. Rhodamine B is applied to investigate the temperature distribution in a straight microchannel and to identify temperature increase due to localized heating in the microchannel [9,10]. Chamarthy *et al*. have applied ratiometric LIF thermometry with Rhodamine B as temperature probe for temperature measurements at T-junction in microchannel devices to observe heat transfer during the mixing of a cold and a hot water flow [11]. In addition to Rhodamine B, various luminescent molecules can be selected and applied in experiments for different temperature ranges with improved temperature sensitivity. Detailed characteristics of luminescent molecules for molecule-based temperature sensor can be found in Ref [12]. With careful calibration, the luminescent intensity can be translated to temperature data for further analysis. Due to the small size of these luminescent molecules, which is usually less than a few nanometers, these molecules can be dispersed in fluid and the mixture can be filled inside the microchannel for fluid temperature measurements. This technique provides global fluid temperature profiles with spatial resolution around a few micrometers using macro photography technique. Additionally, the luminescent molecules can be attached to polymer layer and applied at the surface to acquire surface temperature data for heat transfer analysis. This technique has been successfully applied in a straight PDMS microchannel to acquire both surface and fluid temperature data and perform heat transfer analysis, and the information is beneficial in understanding the microchannel flow inside micro heat exchangers [1]. This work presents the experimental investigation of both temperature and velocity measurements near the 90-degree sharp bend in a microchannel and reveals the temperature variation and corresponded flow pattern around the corner.

2. EXPERIMENTAL

The detailed information regarding molecule-based temperature sensor technique is included in our previous paper [1]. Rhodamine B, which is generally used in TSP and LIF measurements, was selected as the temperature probe to acquire fluid temperature profiles in the PDMS microchannel with a 90-degree sharp bend. It was dispersed in DI water and the mixture served as the temperature-sensitive fluid. The temperature-sensitive fluid was prepared at the ratio of 1mg Rhodamine B to 10ml DI water. The PDMS microchannel was 2 cm long, 200μm wide, and 67μm deep with a 90-degree sharp bend at center. It was made by standard soft-lithography. PDMS (Sylgard 184, Dow Corning, USA) was prepared at the ratio of 10 to 1 for the silicone elastomer and elastomer curing agent. Two circular reservoirs were positioned at the channel inlet and exit to provide uniform and smooth flow inside the microchannel. T-type thermocouples were installed at the inlet and exit reservoirs for monitoring the temperature conditions during the measurements and serving as the reference temperature readout during the in-situ calibration. The surface temperature at the bottom of PDMS microchannel was controlled at 50°C by an electrical heater to provide constant wall temperature. A 7cm long, 5cm wide and 3mm thick copper plate was positioned between the heater and the PDMS microchannel to provide constant and uniform temperature distribution during the measurements. A white base coat was applied on the top surface of the copper plate to cover the machining scratch and enhance the luminescent signal. A thin layer of PDMS was applied on the top of white paint for bonding to the PDMS microchannel. The heater was attached underneath the copper plate and a T-type thermocouple was attached to the surface of copper plate for feed-back temperature control. The temperature distribution on the copper block surface before bonded to the PDMS microchannel was examined at several locations and less than 0.5°C deviation was observed while the surface temperature was controlled at 50°C. The mixture of Rhodamine B and DI water was filled in a syringe then delivered into the microchannel by a syringe pump (KDS 120, KD Scientific). The luminescent images were acquired by a 14 bit high resolution CCD camera (PCO 1600, 1400 × 1600 pixel, PCO). Two UV LED arrays (~ 400nm) provided illumination from the sides for excitation of Rhodamine B. A 550nm long pass optical filter along with a set of extension tube on a 105mm Nikon macro lens were installed on the CCD camera to provide the magnification up to 144μm per pixel and 2700 data points throughout the microchannel.

The Arrhenius equation is commonly used to translate the luminescent intensity to temperature data:

$$\ln \frac{I(T)}{I(T_{ref})} = \frac{E}{R}\left(\frac{1}{T} - \frac{1}{T_{ref}}\right) \tag{1}$$

where E is the Arrhenius activation energy, R is the universal gas constant, $I(T)$ and $I(T_{ref})$ are the intensities acquired at specified temperature and reference temperature during the measurement and calibration. T and T_{ref} are the temperature readings obtained during the measurement and reference condition in the unit of Kelvin, respectively. For practical applications, a high order polynomial equation is generally applied for the calibration.

$$\frac{I(T)}{I(T_{ref})} = F(T / T_{ref}) \tag{2}$$

https://doi.org/10.1017/jmech.2014.60 Published online by Cambridge University Press

The schematic of molecule-based temperature measurements using luminescent molecules dispersed in the fluid inside microchannel is shown in Fig. 1. Figure 2 shows the experimental setup of molecule-based temperature measurements in the microchannel with *x*-*y*-*z* coordinate system used in the data analysis. During the experiment, in-situ calibration and pixel-by-pixel correction method were performed during each measurement to ensure the identical sensors and illumination conditions for both calibration and measurement. The pixel-by-pixel correction method resolves the luminescence deviation observed in microscale luminescent measurements [13]. The algorithm of applying pixel-by-pixel correction method in microscale measurements was reported and the method has been demonstrated as powerful technique in resolving the non-uniformity luminescence issues [14,15]. In this study, the temperature data are presented as the averaged results after taking 100 images in order to reduce the random error introduced by shot noise from the CCD camera and improve the signal to noise ratio. The calibration between luminescent intensity of Rhodamine B and temperature ranging from 24 to 80°C is shown in Fig. 3

3. RESULTS AND DISCUSSION

The temperature profile in the PDMS microchannel with a 90-degree bend was acquired with Rhodamine B and DI water mixture at the flow rate of 12.65ml/hr, as shown in Fig. 4. The distance from the microchannel inlet to the corner is L_{ref} = 1cm which is the same as the distance from the corner to the exit. It is observed that the temperature of the fluid is respectively higher and lower near the out and inner corner of the bend. Overall, the fluid temperature increases gradually toward the downstream direction. Figure 5 shows the temperature variation along the central line of the microchannel from inlet to exit. It should be noted that the temperature measurements using molecule-based temperature sensor were obtained with optical access through the top of microchannel; therefore, the results are depth-integrated temperature of fluid, *i.e.* the bulk fluid temperature (T_m) in the microchannel. This measurement cannot provide the temperature variation along the depth which is expected to gradually increase from bottom to top due to the bottom side heating. The temperature distribution was acquired under constant wall temperature (50°C) thermal boundary condition. The Reynolds number was fixed at 27.66. The fluid was injected into the inlet reservoir where its temperature was around 36°C at the microchannel entrance. The fluid temperature increased to 40°C at the location about 10% of L_{ref} after the entrance. Then it gradually increased to 42°C while approaching to the corner. There was a 2°C temperature increase as the flow passed through the corner, which shows the enhanced heat transfer around this region. After the corner, the fluid temperature continued increasing gradually to 46°C at the location of $x / L_{ref} \fallingdotseq 0.6$.

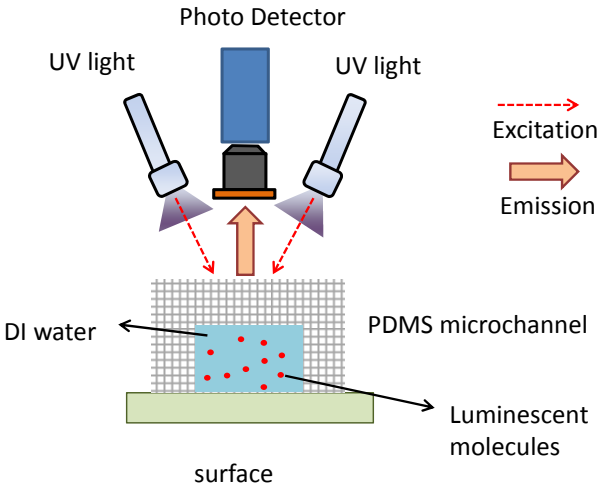


Fig. 1 Schematic of molecule-base temperature measurements in a PDMS microchannel.

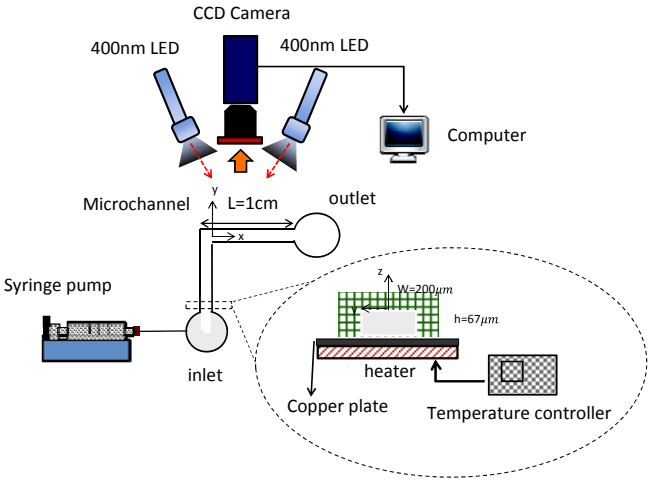


Fig. 2 Experimental setup of molecule-base temperature measurements in the PDMS microchannel.

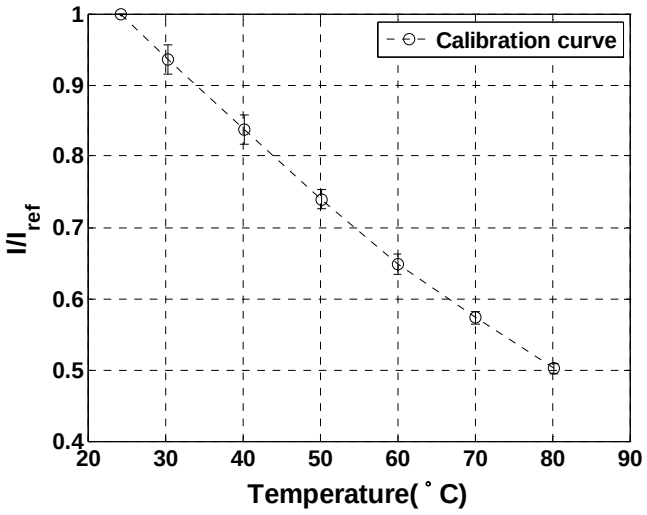


Fig. 3 Calibration curve of Rhodamine *B* luminescent intensity and temperature.

https://doi.org/10.1017/jmech.2014.60 Published online by Cambridge University Press

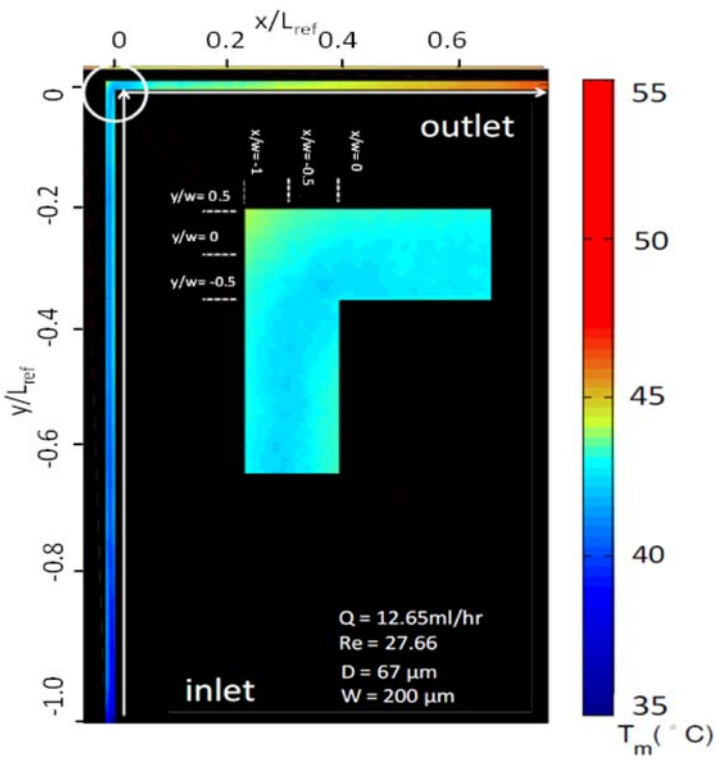


Fig. 4 Temperature contours in the PDMS microchannel around the 90-degree bend at the flow rate of 12.65ml/h (L_{ref} = 1cm).

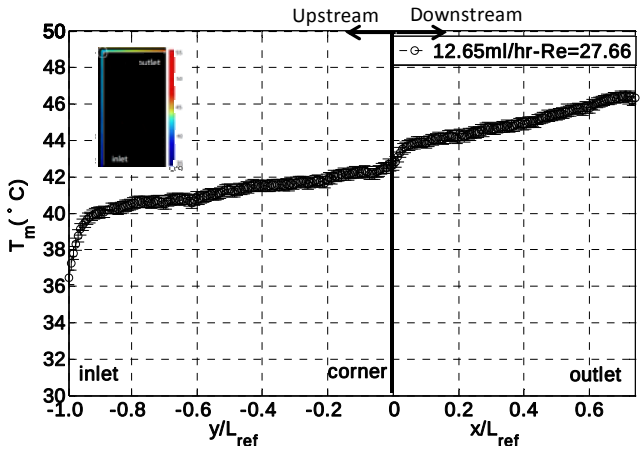


Fig. 5 Temperature distribution along the central line inside microchannel: inlet ($y/L_{ref} = -1.0$), 90 degree bend ($y/L_{ref} = 0$), outlet ($x/L_{ref} = 1$). L_{ref}: 1cm, the distance between inlet and bend as well as from the bend to the outlet.

With the advantages of global measurements using molecule-based temperature sensor, the temperature profiles at the region of interest (which is the corner in this study) could be further examined not only in the axial direction but also lateral direction. To discuss the enhanced heat transfer at the 90-degree bend, the temperature distributions before the corner are presented in Fig. 6. Lateral temperature distributions at different locations upstream of the corner are plotted with normalized location with respect to the channel width ($w = 200\mu m$) starting from inner side wall ($x/w = 0$) to

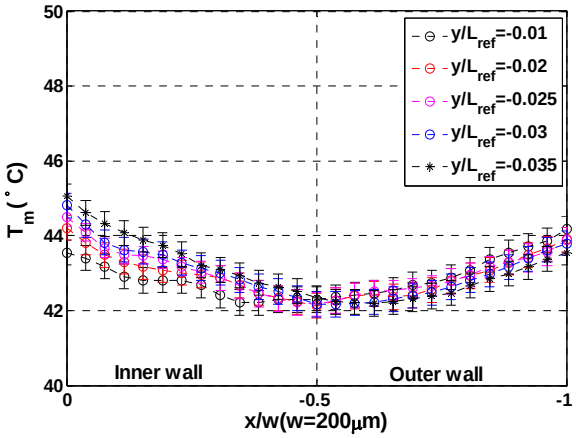


Fig. 6 Lateral temperature distributions acquired at different locations immediately before the 90-degree corner.

the outer side wall ($x/w = -1$). Temperature increase was identified at the area near the outer side whereas the temperature next to the inner wall gradually decreased while the flow was approaching the 90 degree corner from y/L_{ref} of −0.035 to −0.010. Figure 7 shows the temperature evolution at different locations after flow passing the corner from x/L_{ref} of 0.02 to 0.2. The temperature increase after the corner is about 2°C. The above temperature variations result from the helical flow induced by the curvature of the bend and the discussion needs to be correlated with the velocity profiles. Due to the limitation of luminescent-based temperature measurement, only 2-D temperature profiles in the microchannel can be acquired. The temperature variation along the depth cannot be resolved using the current experimental technique.

For discussing the temperature rise after the 90-degree bend, a velocity measurement inside the microchannel around 90-degree bend was carried using micro-PIV technique, the region of interest was focused at the corner and detailed velocity profiles were acquired at different positions along the z-direction (depth). Figure 8(a) shows the averaged velocity profile acquired at the center of the z-direction in microchannel. In Fig. 8(a), the flow velocity at the inner region accelerated when approaching to the corner; meanwhile, the flow velocity at outer region decelerated. The change of flow velocity confirms the observation of the temperature variation aforementioned. After passing the corner, the flow velocity at the inner region decelerated while the flow velocity at outer region accelerated. The change of the flow velocity at inner and outer regions indicates the forming of secondary flow around the corner. To further investigate the secondary flow pattern around the corner, the velocity profiles at different layers along z-directions have been acquired at one hydraulic diameter (D_h) downstream of the corner. The lateral velocity vectors (v) from different z locations are presented to show the pattern of secondary flow as shown in Fig. 8(b). The velocity profiles along the z-direction were acquired at 4μm interval to provide detailed information regarding to the flow pattern.

https://doi.org/10.1017/jmech.2014.60 Published online by Cambridge University Press

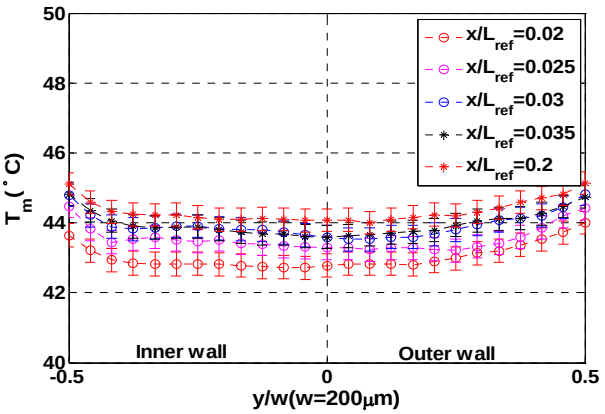


Fig. 7 Lateral temperature distributions acquired at different lateral locations immediately after the 90 degree corner.

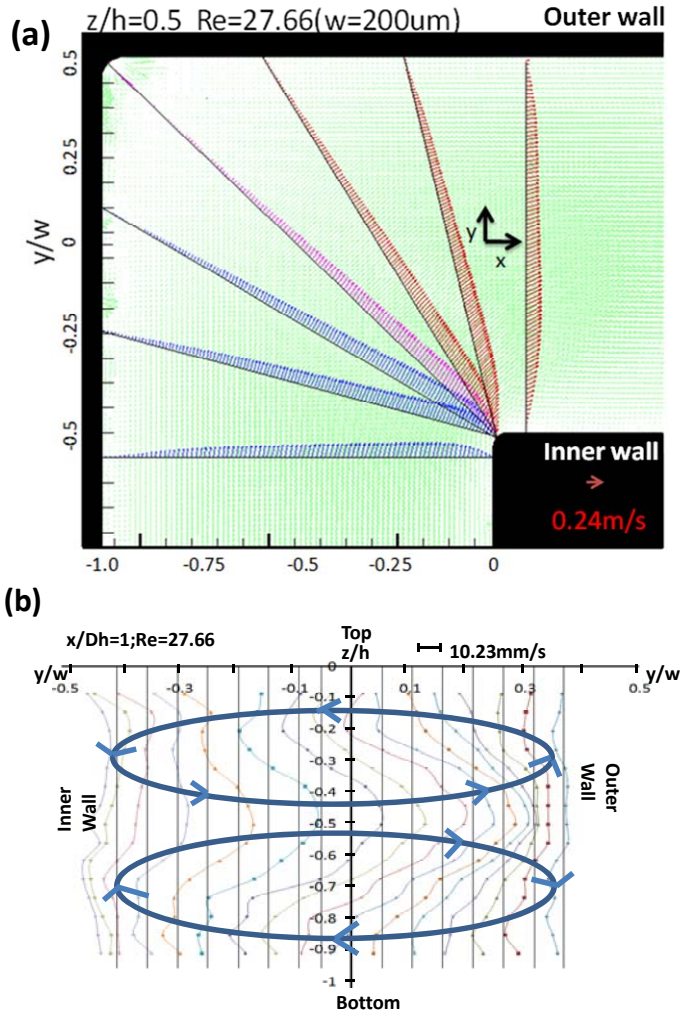


Fig. 8 (a) Averaged velocity profiles (top view) around the corner. (b) Cross-section velocity profiles acquired at one hydraulic diameter downstream of the 90 degree bend ($x/D_h = 1$).

In Fig. 8(b), the *v*-component velocity profiles at different *z* locations are plotted. Each solid line at different *y*/*w* location (thin black line on the figure) represents the zero velocity at the specified *y* location during the measurements. The outer wall is located at *y*/*w* = 0.5 and inner wall at *y*/*w* = –0.5. The *x*, *y*, and *z* locations are normalized by the hydraulic diameter of the microchannel (D_h), the width of microchannel (*w*), and the depth of microchannel (*h*) respectively. Every connected line with data points (thin color line on the figure) in the profile represents the *v*-component velocity acquired at the same *y* location but with data points measured at different *z* locations. The positive and negative *v*-component velocities, which are corresponding to the zero velocity line at each y location, indicate the direction and magnitude of flow velocity. By observing the pattern of velocity profiles at this region, it can be seen that the main flow located at the middle of the channel depth was pushed toward the outer wall due to the centrifugal force while passing the corner, resulting in the aforementioned increase of the fluid temperature near outer wall. After reaching the outer wall, the flow changed the direction and moving back to the center through upper (top) and lower (bottom) regions, therefore, a pair of counter-recirculating flows was generated (thick blue line on the figure). The circulating flow at upper region extends the cold flow to the inner region as shown in Fig 8. The presence of secondary flow pattern helps the flow mixing and heat dissipation from the side walls resulting in the increase of the fluid temperature and, in turn, enhanced heat transfer at the corner.

4. CONCLUSIONS

In this work, temperature profiles have been successfully acquired in a PDMS microchannel with a 90-degree sharp bend using molecule-based temperature sensor. The acquired temperature data reveal the evolution of temperature profiles from entrance to 90-degree bend, where the fluid experiences flow mixing and consequent temperature increase of 2°C. The detailed temperature profiles acquired around the corner show the temperature variations at inner and outer walls in the vicinity of the corner. These temperature evolutions agree with secondary flow patterns identified from the velocity measurement. A pair of counter-rotating circulations was observed at the location of one hydraulic diameter downstream of the corner and it effectively increased the flow mixing and consequently enhanced heat transfer even at the low Reynolds number flow of 27.66 in this study. The temperature and velocity information obtained from current study can be applied to improve the efficiency of micro heat exchanger operated at low Reynolds number.

ACKNOWLEDGEMENTS

The author would like to thank Prof. S. Wereley from Dept. of Mechanical Engineering at Purdue University, USA for the help of EdPIV software for micro-PIV analysis. The author would also like to thank the financial support from NSC project NSC101-2221-E-007-057-MY3.

https://doi.org/10.1017/jmech.2014.60 Published online by Cambridge University Press

REFERENCES

1. Huang, C., Li, C., Wang, H. and Liou, T., "The Application of Temperature-Sensitive Paints for Surface and fluid Temperature Measurements in Both Thermal Developing and Fully Developed Regions of a Microchannel," *Journal of Micromechanics and Microengineering*, **23**, p. 037001, (2013).
2. Harms, T. M., Kazmierczak, M. J. and Gerner, F. M., "Developing Convective Heat Transfer in Deep Rectangular Microchannels," *International Journal of Heat and Fluid Flow*, **20**, pp. 149–157 (1999).
3. Rosaguti, N. R., Fletcher, D. F. and Haynes, B. S., "Laminar Flow and Heat Transfer in a Periodic Serpentine Channel with Semi-Circular Cross-Section," *International Journal of Heat and Mass Transfer*, **49**, pp. 2912–2923 (2006).
4. Sun, Y. J., Jian, Y. J., Chang, L. and Liu, Q. S., "Thermally Fully Developed Electroosmotic Flow of Power-Law Fluids in a Circular Microchannel," *Journal of Mechanics*, **29**, pp. 609–616 (2013).
5. Peng, X. F. and Piao, Y., "Characteristics of Fluid Flow and Convection Heat Transfer in Microchannels," *Advances in Fluid Mechanics IV*, pp. 85–94 (2002).
6. Gau, C. and Ko, H. S., "Local Heat Transfer Process and Pressure Drop in a Microchannel Integrated with Arrays of Temperature and Pressure Sensors," *Microfluid Nanofluid*, **10**, pp. 563–577 (2011).
7. Huang, C., Gregory, J., Nagai, H., Asai, K. and Sullivan, J., "Molecular Sensors in Microturbine Measurement," *International Mechanical Engineering Congress & Exposit*ion, Chicago, Illinois, USA (2006).
8. Natrajan, V. K. and Christensen, K. T., "Non-Intrusive Measurements of Convective Heat Transfer in Smooth- and Rough-Wall Microchannels: Laminar Flow," *Experiments in Fluids*, **49**, pp. 1021–1037 (2010).
9. Fu, R., Xu, B. and Li, D., "Study of the Temperature Field in Microchannels of a PDMS Chip with Embedded Local Heater Using Temperature-Dependent Fluorescent Dye," *International Journal of Thermal Sciences*, **45**, pp. 841–847 (2006).
10. Samy, R., Glawdel, T. and Ren, C. L., "Method for Microfluidic Whole-Chip Temperature Measurement Using Thin-Film Poly(Dimethylsiloxane) / Rhodamine b," *Analytical Chemistry*, **80**, pp. 369–375 (2008).
11. Chamarthy, P., Garimella, S. V. and Wereley, S. T., "Measurement of the Temperature Non-Uniformity in a Microchannel Heat Sink Using Microscale Laser-Induced Fluorescence," *International Journal Heat and Mass Transfer*, **53**, pp. 3275–3283 (2010).
12. Liu, T. and Sullivan, J. P., *Pressure and Temperature Sensitive Paints*, Springer-Verlag: Berlin, Germany (2004).
13. Huang, C. Y., Lai, C. M. and Li, J. S., "Applications of Pixel-By-Pixel Calibration Method in Microscale Measurements with Pressure-Sensitive Paint," *Journal of Microelectromechanical Systems*, **21**, pp. 1090–1097 (2012).
14. Huang, C. Y. and Lai, C. M., "Pressure Measurements with Molecule-Based Pressure Sensors in Straight and Constricted PDMS Microchannels," *Journal of Micromechanics and Microengineering*, **22**, p.065021 (2012).
15. Huang, C., Gregory, J. and Sullivan, J., "Microchannel Pressure Measurements Using Molecular Sensors," *Journal of Microelectromechanical Systems*, **16**, pp. 777–785 (2007).

(Manuscript received May 2, 2014,
accepted for publication July 2, 2014.)

https://doi.org/10.1017/jmech.2014.60 Published online by Cambridge University Press